Hindawi
Shock and Vibration
Volume 2022, Article ID 7515080, 13 pages
https://doi.org/10.1155/2022/7515080

Research Article

Dynamical Behavior of Fractional-Order Delayed Feedback Control on the Mathieu Equation by Incremental Harmonic Balance Method

Shaofang Wen,[1,2] **Yongjun Shen**,[1,3] **Jiangchuan Niu**,[1,3] **and Yunfei Liu**[2]

[1]*State Key Laboratory of Mechanical Behavior and System Safety of Traffic Engineering Structures, Shijiazhuang Tiedao University, Shijiazhuang 050043, China*
[2]*Key Laboratory of Traffic Safety and Control of Hebei Province, Shijiazhuang Tiedao University, Shijiazhuang 050043, China*
[3]*School of Mechanical Engineering, Shijiazhuang Tiedao University, Shijiazhuang 050043, China*

Correspondence should be addressed to Shaofang Wen; wsf39811@163.com

Received 27 January 2022; Revised 23 May 2022; Accepted 20 June 2022; Published 19 July 2022

Academic Editor: Marcos Silveira

In this study, the dynamical analysis of the Mathieu equation with multifrequency excitation under fractional-order delayed feedback control is investigated by the incremental harmonic balance method (IHBM). IHBM is applied to the fractional-order delayed feedback control system, and the general formulas of the first-order approximate periodic solution for the Mathieu equation are derived. Caputo's definition is adopted to process the fractional-order delayed feedback term. The general formulas of this system are suitable for not only the weakly but also the strongly nonlinear fractional-order system. Through the analysis of the general formulas of this system, it shows that fractional-order delayed feedback control has two functions, which are velocity delayed feedback control and displacement delayed feedback control. Next, the numerical simulation of the system is carried out. The comparison between the approximate analytical solution and the numerical iterative result is made, and the accuracy of the approximate analytical result by IHBM is proved to be high. At last, the effects of the time delay, feedback coefficient, and fractional order are investigated, respectively. It is generally known that time delay is common and inevitable in the control system. But the fractional order can be used to adjust the influence caused by time delay in fractional-order delayed feedback control. Those new system characteristics will provide theoretical guidance to the design and the control of this kind system.

1. Introduction

The definition of fractional calculus has existed for more than 300 years. Fractional calculus has many advantages. For example, it could better reflect the viscoelastic and the memory properties of materials, and also provide better control performance. With the development of science and the increase in the demand of complex engineering application, a lot of scholars in different research fields are attracted by fractional calculus [1–5].

At present, fractional calculus has played a very important role in different fields, such as electrochemistry, signal processing, bioengineering, mechanics, and control. The research of basic theory has been greatly improved on fractional calculus, and the achievement of the basic theoretical research mainly focuses on the following aspects: qualitative analysis, numerical calculation, and analytical research [6–10]. For example, Wang et al. [11, 12] studied the dynamics of the linear fractional-order system under external excitation and proved that the fractional-order feedback can not only adjust the damping force but also adjust the elastic force. Then, the stabilities of the various fractional-order systems are studied, and an effective judging method for the stability of the fractional-order system is proposed. Trigeassou et al. [13] investigated the stability of the fractional-order system by Lyapunov theory. Li et al. [14, 15] presented some higher-order iterative algorithms of fractional-order differential equations based on the Simpson method and put forward some numerical calculation methods of fractional-order partial differential equations.

Ebaid et al. [16] developed a new approach to solve a class of first-order fractional initial value problems based on Riemann–Liouville fractional derivative. Failla et al. [17] proposed a numerical method to investigate the dynamical response of the fractional-order system with random excitation. Shen et al. [18, 19] studied the approximate analytical solutions of several fractional-order systems by the improved average method and the dynamics of the strongly nonlinear fractional-order system by the improved incremental harmonic balance method.

In the engineering application, the system model is generally complex, and it is often affected by multifrequency excitation and strong nonlinearity. At this moment, the system cannot be regarded as a perturbed system for its derived linear system because the strong nonlinearity will seriously affect the stability of the periodic solution. Those classical perturbation methods for the weakly nonlinear system are used to study the strongly nonlinear problems will cause enormous error [20, 21].

In the present survey, some efficient analytical methods and numerical integration methods for the strongly nonlinear system have been presented now. For the numerical integration method, because of its slow convergence speed, it is very difficult to analyze the effects of those parameters in complex dynamical systems. However, some efficient analytical methods, such as the generalized multiple-scale method with its improved version, the perturbation-incremental method and the homotopy analysis method [22–25] could provide satisfactory results for those strongly nonlinear oscillators in some complex engineering. IHBM is a classical, effective, and semianalytical method with many advantages. For example, it could be used to deal with strongly and weakly nonlinear systems at the same time [26–28], and its convergence speed is very fast. Moreover, the solution with higher accuracy can be obtained through the increasing of the solution order based on IHBM. That means that IHBM can be applied into those different nonlinear systems and also is widely used in the engineering field.

The application of fractional calculus in the control system is also unique. Chen et al. [29] proposed a new fractional-order control method for the four-wheel steering system, which improved the transient response of the vehicle in the steering process. Chen et al. [30] studied the nonlinear dynamical characteristics of the fractional-order Duffing system with random excitation, and presented an efficient bifurcation control method based on the fractional-order PIλDμ feedback controller. Avci et al. [31] proposed spectral formulation for a fractional optimal control problem defined in spherical coordinates. The dynamical response of the Mathieu–Duffing oscillator with fractional-order delayed feedback control is studied by the average method, and it can be concluded that fractional-order delayed feedback control can better control the dynamical characteristics of the system [19]. As we all know, time delay is inevitable in control engineering. The dynamical phenomena of the system under the combined action of parametric excitation and multifrequency excitation are more complicated [32–34]. Accordingly, the general formulas of the Mathieu equation with multifrequency excitation under fractional-order delayed feedback control based on IHBM are obtained in the following. The dynamical analysis of the Mathieu equation with multifrequency excitation under fractional-order delayed feedback control is investigated by the obtained general formulas. Also, the general formulas can be used to study a variety of complex strongly nonlinear systems.

In this paper, the Mathieu equation with multifrequency excitation is presented in Section 2. In addition, the general formulas of the Mathieu equation with multifrequency excitation under fractional-order delayed feedback control are derived by IHBM in Section 2. Then, in Section 3, the numerical result is studied and the correctness of the result by IHBM is verified by numerical simulation. In Section 4, the influence of the fractional order, the feedback gain coefficient, and time delay is investigated, respectively. From the analysis of the general formulas and the simulation results, the correlation between the fractional order and time delay is studied. Fractional order and time delay can be adjusted with each other, so fractional-order delayed feedback control will provide a wider design and adjustment space in the control system. At last, the main conclusions are drawn.

2. The General Formulas by IHBM

In this paper, the Mathieu equation with multifrequency excitation is considered. At first, this system under fractional-order delayed feedback control is

$$\begin{aligned}\frac{\mathrm{d}^2x(t)}{\mathrm{d}t^2}+\mu\frac{\mathrm{d}x(t)}{\mathrm{d}t}+(1+2\varepsilon\cos\omega t)x(t)+U(t)\\ =F_0-\sum_{k=1}^{L}F_k\cos k\omega t,\end{aligned}\tag{1}$$

where $x(t)$ is the system displacement, μ is the damping coefficient, $2\varepsilon\cos\omega t$ is the periodic time-varying stiffing coefficient, and F_0 and $\sum_{k=1}^{L}F_k\cos k\omega t$ are the constant excitation and multifrequency excitation, respectively. $U(t)$ is fractional-order delayed feedback control. Here, $U(t)=F_pD^p[x(t-\tau_1)]$, τ_1 is the time delay, F_p is the feedback gain coefficient, and $D^p[x(t-\tau_1)]$ represents p-order $(0\le p\le 2)$ derivative of $x(t-\tau_1)$ to t. When $p=0$, fractional-order delayed feedback becomes displacement delayed feedback. When $p=1$, fractional-order delayed feedback becomes velocity delayed feedback.

At present, there are several most frequently used definitions for fractional calculus, such as Grünwald–Letnikov, Riemann–Liouville, and Caputo definitions, which are equivalent under some conditions [1, 2]. Here, Caputo's definition is adopted as

$$D^p[x(t)]=\frac{1}{\Gamma(1-p)}\int_0^t\frac{x'(u)}{(t-u)^p}\mathrm{d}u,\tag{2}$$

where $\Gamma(y)$ is Gamma function satisfying $\Gamma(y+1)=y\Gamma(y)$.

Let $\tau=\omega t$, $\tau_0=\omega\tau_1$, and equation (1) becomes

$$\omega^2\ddot{x}(\tau)+\omega\mu\dot{x}(\tau)+(1+2\varepsilon\cos\tau)x(\tau)+F_p\omega^p D_\tau^p[x(\tau-\tau_0)] = F_0+\sum_{k=1}^{L}F_k\cos k\tau. \tag{3}$$

The symbol "·" represents the derivative with respect to τ. The periodic solution with N-order harmonic terms of equation (3) is expressed as follows:

$$x_0 = a_0+\sum_{n=1}^{N}[a_n\cos(n\tau)+b_n\sin(n\tau)], \tag{4a}$$

and

$$\Delta x_0 = \Delta a_0+\sum_{n=1}^{N}[\Delta a_n\cos(n\tau)+\Delta b_n\sin(n\tau)]. \tag{4b}$$

Substituting $x = x_0+\Delta x_0$ into equation (3), using Taylor series expression, and omitting the higher-order terms of the small increment Δx, one can obtain the differential equation as

$$\begin{aligned}\omega^2\Delta\ddot{x}_0+\omega\mu\Delta\dot{x}_0+(1+2\varepsilon\cos\tau)\Delta x_0 &+F_p\omega^p D_\tau^p[\Delta x_0(\tau-\tau_0)]\\ &= F_0-\sum_{k=1}^{L}F_k\cos k\tau\\ &-F_p\omega^p D_\tau^p[\Delta x_0(\tau-\tau_0)]-f_0,\end{aligned} \tag{5}$$

where $f_0 = \omega^2\ddot{x}_0+\omega\mu\dot{x}_0+(1+2\varepsilon\cos\tau)x_0$.

Defining the following vectors

$$X = [1,\ \cos\tau,\ \cos 2\tau,\dots\ \cos n\tau,\ \sin\tau,\ \sin 2\tau,\dots\ \sin n\tau], \tag{6a}$$

$$X(\tau-\tau_0) = \begin{bmatrix}1,\ \cos(\tau-\tau_0),\ \cos(2\tau-\tau_0),\dots\ \cos(n\tau-\tau_0),\\ \sin(\tau-\tau_0),\ \sin(2\tau-\tau_0),\dots\ \sin(n\tau-\tau_0)\end{bmatrix}, \tag{6b}$$

$$A_0 = [a_0,a_1,\dots a_n,b_1,b_2,\dots b_n]^T, \tag{6c}$$

$$\Delta A_0 = [\Delta a_0,\Delta a_1,\dots\Delta a_n,\Delta b_1,\Delta b_2,\dots\Delta b_n]^T, \tag{6d}$$

one can get

$$\begin{aligned}x_0 &= XA_0,\\ \Delta x_0 &= X\Delta A_0,\\ x_0(\tau-\tau_0) &= X(\tau-\tau_0)A_0,\\ \Delta x_0(\tau-\tau_0) &= X(\tau-\tau_0)\Delta A_0.\end{aligned} \tag{6e}$$

Based on Galerkin's procedure [26, 27], the integral for equation (5) is deduced in the following. In this procedure, fractional-order delayed feedback item is an aperiodic function, so the time terminal is selected as $T=\infty$. The other items of equation (5) are periodic functions with a period of 2π, so the time terminal is selected as $T = 2\pi$. Accordingly, one can get the following equations:

$$\begin{aligned}\frac{1}{2\pi}\int_0^{2\pi}\delta(\Delta x_0)\left[\omega^2\Delta\ddot{x}_0+\omega\mu\Delta\dot{x}_0+(1+2\varepsilon\cos\tau)\Delta x_0\right]\mathrm{d}\tau &\\ +\frac{1}{T}\int_0^{T}\delta(\Delta x_0)\left\{F_p\omega^p D_\tau^p[\Delta x_0(\tau-\tau_0)]\right\}\mathrm{d}\tau &\\ =\frac{1}{2\pi}\int_0^{2\pi}\delta(\Delta x_0)\left[F_0-\sum_{k=1}^{L}F_k\cos k\tau-f_0\right]\mathrm{d}\tau &\\ -\frac{1}{T}\int_0^{T}\delta(\Delta x_0)\left\{F_p\omega^p D_\tau^p[x_0(\tau-\tau_0)]\right\}\mathrm{d}\tau.&\end{aligned} \tag{7}$$

Rearrange equation (7), and it yields

$$\begin{aligned}\delta(\Delta A_0)^T\left\{\frac{1}{2\pi}\int_0^{2\pi}X^T\left[\omega^2\ddot{X}+\omega\mu\dot{X}+(1+2\varepsilon\cos\tau)X\right]\mathrm{d}\tau\right\}\Delta A_0 &\\ +\delta(\Delta A_0)^T\left\{\frac{1}{T}\int_0^{T}X^T\left\{F_p\omega^p D_\tau^p[X(\tau-\tau_0)]\right\}\mathrm{d}\tau\right\}\Delta A_0 &\\ =\delta(\Delta A_0)^T\left\{\frac{1}{2\pi}\int_0^{2\pi}X^T\left[F_0-\sum_{k=1}^{L}F_k\cos k\tau-f_0\right]\mathrm{d}\tau\right\} &\\ -\delta(\Delta A_0)^T\left\{\frac{1}{T}\int_0^{T}X^T F_p\omega^p D_\tau^p[x_0(\tau-\tau_0)]\mathrm{d}\tau\right\}.&\end{aligned} \tag{8}$$

Then, obtaining the $2N+1$ linearized equations about ΔA_0

$$M\Delta A_0 = R, \tag{9}$$

where

$$M = M_1+M_2^p, \tag{10a}$$

$$M_1 = \frac{1}{2\pi}\int_0^{2\pi}X^T\left[\omega^2\ddot{X}+\omega\mu\dot{X}+(1+2\varepsilon\cos\tau)X\right]\mathrm{d}\tau, \tag{10b}$$

$$M_2^p = \frac{1}{T}\int_0^{T}X^T F_p\omega^p D_\tau^p[X(\tau-\tau_0)]\mathrm{d}\tau, \tag{10c}$$

$$R = R_1+R_2^p, \tag{10d}$$

$$R_1 = \frac{1}{2\pi}\int_0^{2\pi}X^T\left[F_0-\sum_{k=1}^{L}F_k\cos k\tau-f_0\right]\mathrm{d}\tau, \tag{10e}$$

$$R_2^p = \frac{1}{T}\int_0^{T}X^T F_p\omega^p D_\tau^p[x_0(\tau-\tau_0)]\mathrm{d}\tau, \tag{10f}$$

and expanding to matrix forms

$$M_1 = \begin{bmatrix} [M_{11}] & [M_{12}] \\ [M_{21}] & [M_{22}] \end{bmatrix}, \quad R_1 = \begin{bmatrix} [R_{10}] \\ [R_{11}] \\ [R_{12}] \end{bmatrix}, \tag{11}$$

one could obtain the explicit expression of M_1 and R_1 as follows:

$$[M_{11}] = \begin{cases} \delta_{ij} + \varepsilon\left[\dfrac{\sin(1+i-j)\theta}{(1+i-j)\theta} + \dfrac{\sin(1-i+j)\theta}{(1-i+j)\theta}\right], & \begin{cases} i = 0, j = 0, 1, \ldots, N, \\ j = 0, i = 1, \ldots, N, \end{cases} \\ -\dfrac{1}{2}\delta_{ij} j^2\omega^2 + \dfrac{\delta_{ij}}{2} + \dfrac{\varepsilon}{2}\left[\dfrac{\sin(1+i-j)\theta}{(1+i-j)\theta} + \dfrac{\sin(1-i+j)\theta}{(1-i+j)\theta}\right], & i = 1, \ldots, N, j = 1, \ldots, N, \end{cases} \tag{12a}$$

$$[M_{12}] = \frac{1}{2}\mu\delta_{ij} j\omega, \quad i = 0, 1, \ldots, N, j = 1, \ldots, N, \tag{12b}$$

$$[M_{21}] = -\frac{1}{2}\mu\delta_{ij} j\omega, \quad i = 1, \ldots, N, j = 0, 1, \ldots, N, \tag{12c}$$

$$[M_{22}] = -\frac{1}{2}\delta_{ij} j^2\omega^2 + \frac{\delta_{ij}}{2} + \frac{\varepsilon}{2}\left[\frac{\sin(1+i-j)\theta}{(1+i-j)\theta} + \frac{\sin(1-i+j)\theta}{(1-i+j)\theta}\right], \quad i = 1, \ldots, N, j = 1, \ldots, N, \tag{12d}$$

$$[R_{10}] = F_0 - a_0 + R_{10i}^{CJ}, i = 0, \tag{12e}$$

$$[R_{11}] = \begin{cases} \dfrac{1}{2}\left[f_i + \left(i^2\omega^2 a_i - \mu i\omega b_i\right)\right] - \dfrac{a_i}{2} + R_{11i}^{CJ}, i \le L, \\ \dfrac{1}{2}\left[i^2\omega^2 a_i - \mu i\omega b_i\right] - \dfrac{a_i}{2} + R_{11i}^{CJ}, i > L, \end{cases}, \quad i = 1, \ldots, N, \tag{12f}$$

$$[R_{12}] = \frac{1}{2}\left(i^2\omega^2 b_i + \mu i\omega a_i\right) - \frac{b_i}{2} + R_{12i}^{CJ}, \quad i = 1, \ldots, N, \tag{12g}$$

where

$$\begin{aligned} R_{10i}^{CJ} &= R_{11i}^{CJ} \\ &= -\sum_{j=0}^{N}\frac{\varepsilon}{2}a_j\left[\frac{\sin(1+i+j)\theta}{(1+i+j)\theta} + \frac{\sin(1+i-j)\theta}{(1+i-j)\theta} + \frac{\sin(1-i+j)\theta}{(1-i+j)\theta} + \frac{\sin(1-i-j)\theta}{(1-i-j)\theta}\right], \\ R_{12i}^{CJ} &= -\sum_{j=1}^{N}\frac{\varepsilon}{2}b_j\left[\frac{\sin(1+i+j)\theta}{(1+i+j)\theta} + \frac{\sin(1+i-j)\theta}{(1+i-j)\theta} + \frac{\sin(1-i+j)\theta}{(1-i+j)\theta} + \frac{\sin(1-i-j)\theta}{(1-i-j)\theta}\right], \end{aligned} \tag{13}$$

where δ_{ij} is the Kronecker symbol, and the value of θ is 2π.

Then, the integration process of fractional-order delayed feedback is presented. M_2^p and R_2^p are the Jacobi matrix and the corrective vector, respectively, and the forms are as follows:

$$M_2^p = \begin{bmatrix} [M_{11}]^p & [M_{12}]^p \\ [M_{21}]^p & [M_{22}]^p \end{bmatrix}, \quad R_2^p = \begin{bmatrix} R_{200}^p \\ R_{21i}^p \\ R_{22i}^p \end{bmatrix}, \tag{14}$$

where

$$[M_{11}]_{ij}^{p} = \lim_{T\longrightarrow\infty} \frac{1}{T}\int_0^T F_p\omega^p \cos i\tau D_\tau^p[\cos(j\tau-\tau_0)]\mathrm{d}\tau, \quad i=0,1,\ldots,N, j=0,1,\ldots,N, \tag{15a}$$

$$[M_{12}]_{ij}^{p} = \lim_{T\longrightarrow\infty} \frac{1}{T}\int_0^T F_p\omega^p \cos i\tau D_\tau^p[\sin(j\tau-\tau_0)]\mathrm{d}\tau, \quad i=0,1,\ldots,N, j=1,\ldots,N, \tag{15b}$$

$$[M_{21}]_{ij}^{p} = \lim_{T\longrightarrow\infty} \frac{1}{T}\int_0^T F_p\omega^p \sin i\tau D_\tau^p[\cos(j\tau-\tau_0)]\mathrm{d}\tau, \quad i=1,\ldots,N, j=0,1,\ldots,N, \tag{15c}$$

$$[M_{22}]_{ij}^{p} = \lim_{T\longrightarrow\infty} \frac{1}{T}\int_0^T F_p\omega^p \sin i\tau D_\tau^p[\sin(j\tau-\tau_0)]\mathrm{d}\tau, \quad i=1,\ldots,N, j=1,\ldots,N, \tag{15d}$$

$$R_{200}^{p} = \lim_{T\longrightarrow\infty} -\frac{1}{T}\int_0^T \left\{F_p\omega^p D_\tau^p[x_0(\tau-\tau_0)]\right\}\mathrm{d}\tau, \tag{15e}$$

$$R_{21i}^{p} = \lim_{T\longrightarrow\infty} -\frac{1}{T}\int_0^T \left\{F_p\omega^p D_\tau^p[x_0(\tau-\tau_0)]\cos i\tau\right\}\mathrm{d}\tau, \quad i=1,\ldots,N, \tag{15f}$$

$$R_{22i}^{p} = \lim_{T\longrightarrow\infty} -\frac{1}{T}\int_0^T \left\{F_p\omega^p D_\tau^p[x_0(\tau-\tau_0)]\sin i\tau\right\}\mathrm{d}\tau, \quad i=1,\ldots,N. \tag{15g}$$

According to equations (2) and (15a), it can be written as

$$\begin{aligned}[M_{11}]_{ij}^{p} &= \lim_{T\longrightarrow\infty} \frac{1}{T}\int_0^T F_p\omega^p \cos i\tau D_\tau^p[\cos(j\tau-\tau_0)]\mathrm{d}\tau \\ &= \lim_{T\longrightarrow\infty} \frac{1}{T}\int_0^T F_p\omega^p \cos i\tau\left[\frac{1}{\Gamma(1-p)}\int_0^\tau \frac{-j\sin(ju-\tau_0)}{(\tau-u)^p}\mathrm{d}u\right]\mathrm{d}\tau.\end{aligned} \tag{16}$$

Letting $s=\tau-u$ and $du=-ds$, and substituting into equation (16), one can get

$$\begin{aligned}[M_{11}]_{ij}^{p} &= \frac{-jF_p\omega^p}{\Gamma(1-p)}\lim_{T\longrightarrow\infty}\frac{1}{T}\int_0^T \cos i\tau\left[\int_0^\tau \frac{\sin(j\tau-\tau_0-js)}{s^p}\mathrm{d}s\right]\mathrm{d}\tau \\ &= \frac{-jF_p\omega^p}{\Gamma(1-p)}\lim_{T\longrightarrow\infty}\frac{1}{T}\int_0^T\left[\cos i\tau\,\sin(j\tau-\tau_0)\int_0^\tau \frac{\cos js}{s^p}\mathrm{d}s\right]\mathrm{d}\tau \\ &\quad -\frac{-jF_p\omega^p}{\Gamma(1-p)}\lim_{T\longrightarrow\infty}\frac{1}{T}\int_0^T\left[\cos i\tau\,\cos(j\tau-\tau_0)\int_0^\tau \frac{\sin js}{s^p}\mathrm{d}s\right]\mathrm{d}\tau.\end{aligned} \tag{17}$$

From equation (17), it could be found the expression for equation (17) has two integrals. Defining the first integral as A_1 and the second integral as A_2, and integrating it by parts, respectively, one have

$$\begin{aligned} A_1 &= \frac{-jF_p\omega^p}{\Gamma(1-p)}\lim_{T\longrightarrow\infty}\frac{1}{T}\int_0^T\left\{\frac{1}{2}\left[\sin(i\tau+j\tau-\tau_0)-\sin(i\tau-j\tau+\tau_0)\right]\int_0^\tau\frac{\cos js}{s^p}\mathrm{d}s\right\}\mathrm{d}\tau \\ &= \frac{jF_p\omega^p}{2\Gamma(1-p)}\lim_{T\longrightarrow\infty}\frac{1}{T}\left[\frac{\cos(i\tau+j\tau-\tau_0)}{(i+j)}-\frac{\cos(i\tau-j\tau+\tau_0)}{(i-j)}\right]\int_0^\tau\frac{\cos js}{s^p}\mathrm{d}s\Bigg|_0^T \\ &\quad -\frac{jF_p\omega^p}{2\Gamma(1-p)}\lim_{T\longrightarrow\infty}\frac{1}{T}\int_0^T\left[\frac{\cos(i\tau+j\tau-\tau_0)}{(i+j)}-\frac{\cos(i\tau-j\tau+\tau_0)\tau}{(i-j)}\right]\frac{\cos j\tau}{\tau^p}\mathrm{d}\tau, \end{aligned} \tag{18a}$$

$$\begin{aligned} A_2 &= -\frac{-jF_p\omega^p}{\Gamma(1-p)}\lim_{T\longrightarrow\infty}\frac{1}{T}\int_0^T\left\{\frac{1}{2}\left[\cos(i\tau+j\tau-\tau_0)+\cos(i\tau-j\tau+\tau_0)\right]\int_0^\tau\frac{\sin js}{s^p}ds\right\}\mathrm{d}\tau \\ &= \frac{jF_p\omega^p}{2\Gamma(1-p)}\lim_{T\longrightarrow\infty}\frac{1}{T}\left[\frac{\sin(i\tau+j\tau-\tau_0)}{(i+j)}+\frac{\sin(i\tau-j\tau+\tau_0)}{(i-j)}\right]\int_0^\tau\frac{\sin js}{s^p}\mathrm{d}s\Bigg|_0^T \\ &\quad -\frac{jF_p\omega^p}{2\Gamma(1-p)}\lim_{T\longrightarrow\infty}\frac{1}{T}\int_0^T\left[\frac{\sin(i\tau+j\tau-\tau_0)}{(i+j)}+\frac{\sin(i\tau-j\tau+\tau_0)}{(i-j)}\right]\frac{\sin j\tau}{\tau^p}\mathrm{d}\tau. \end{aligned} \tag{18b}$$

To simplify the process, we define the first part of equation (18a) as A_{11}, the second part of equation (18a) as A_{12}, the first part of equation (18b) as A_{21}, and the second part of equation (18b) as A_{22}. Here, two basic formulas [17] are introduced

$$\lim_{T\longrightarrow\infty}\int_0^T\frac{\sin(jt)}{t^p}\mathrm{d}t = j^{p-1}\Gamma(1-p)\cos\left(\frac{p\pi}{2}\right), \tag{19a}$$

$$\lim_{T\longrightarrow\infty}\int_0^T\frac{\cos(jt)}{t^p}\mathrm{d}t = j^{p-1}\Gamma(1-p)\sin\left(\frac{p\pi}{2}\right). \tag{19b}$$

According to equation (19b), we can get

$$\begin{aligned} A_{11} &= \frac{jF_p\omega^p}{2\Gamma(1-p)}\lim_{T\longrightarrow\infty}\frac{1}{T}\left[\frac{\cos(i\tau+j\tau-\tau_0)}{(i+j)}-\frac{\cos(i\tau-j\tau+\tau_0)}{(i-j)}\right]\int_0^\tau\frac{\cos js}{s^p}\mathrm{d}s\Bigg|_0^T \\ &= \frac{F_p\omega^p j^p\sin(p\pi/2)}{2}\lim_{T\longrightarrow\infty}\frac{1}{T}\left[\frac{\cos(iT+jT-\tau_0)}{(i+j)}-\frac{\cos(iT-jT+\tau_0)}{(i-j)}\right] \\ &= \frac{F_p\omega^p j^p\sin(p\pi/2)}{2}\lim_{T\longrightarrow\infty}\frac{1}{T}\left\{\begin{array}{l}\dfrac{\cos[(i+j)T]\cos(\tau_0)}{(i+j)}+\dfrac{\sin[(i+j)T]\sin(\tau_0)}{(i+j)} \\ -\dfrac{\cos[(i-j)T]\cos(\tau_0)}{(i+j)}+\dfrac{\sin[(i-j)T]\sin(\tau_0)}{(i-j)}\end{array}\right\} \\ &= \left\{\begin{array}{l}0, i\neq j, \\ \dfrac{F_p\omega^p j^p\sin(p\pi/2)\sin(\tau_0)}{2}, i=j,\end{array}\right. \end{aligned} \tag{20a}$$

$$A_{12} = -\frac{jF_p\omega^p}{2\Gamma(1-p)}\lim_{T\longrightarrow\infty}\frac{1}{T}\int_0^T\left[\frac{\cos(i\tau+j\tau-\tau_0)}{(i+j)}-\frac{\cos(i\tau-j\tau+\tau_0)\tau}{(i-j)}\right]\frac{\cos j\tau}{\tau^p}\mathrm{d}\tau = 0. \tag{20b}$$

According to equation (19a), we can get

$$\begin{aligned}
A_{21} &= \frac{jF_p\omega^p}{2\Gamma(1-p)}\lim_{T\longrightarrow\infty}\frac{1}{T}\left[\frac{\sin(i\tau+j\tau-\tau_0)}{(i+j)}+\frac{\sin(i\tau-j\tau+\tau_0)}{(i-j)}\right]\int_0^{\tau}\frac{\sin js}{s^p}\mathrm{d}s\Bigg|_0^T \\
&= \frac{F_p\omega^p j^p\cos(p\pi/2)}{2}\lim_{T\longrightarrow\infty}\frac{1}{T}\left[\frac{\sin(iT+jT-\tau_0)}{(i+j)}+\frac{\sin(iT-jT+\tau_0)}{(i-j)}\right] \\
&= \frac{F_p\omega^p j^p\cos(p\pi/2)}{2}\lim_{T\longrightarrow\infty}\frac{1}{T}\left\{\begin{array}{l}\dfrac{\sin[(i+j)T]\cos(\tau_0)}{(i+j)}-\dfrac{\cos[(i+j)T]\sin(\tau_0)}{(i+j)} \\ +\dfrac{\sin[(i-j)T]\cos(\tau_0)}{(i-j)}+\dfrac{\cos[(i-j)T]\sin(\tau_0)}{(i-j)}\end{array}\right\} \\
&= \begin{cases} 0, & i\neq j, \\ \dfrac{F_p\omega^p j^p\cos(p\pi/2)\cos(\tau_0)}{2}, & i=j,\end{cases}
\end{aligned} \tag{21a}$$

$$A_{22} = -\frac{jF_p\omega^p}{2\Gamma(1-p)}\lim_{T\longrightarrow\infty}\frac{1}{T}\int_0^T\left[\frac{\sin(i\tau+j\tau-\tau_0)}{(i+j)}+\frac{\sin(i\tau-j\tau+\tau_0)}{(i-j)}\right]\frac{\sin j\tau}{\tau^p}\mathrm{d}\tau = 0. \tag{21b}$$

Combining equations (17), (18a), (18b), (20a), (20b), (21a), and (21b) we obtain the explicit expression of $[M_{11}]^p$

$$[M_{11}]_{ij}^p = \begin{cases} 0, & i\neq j, \\ \dfrac{F_p\omega^p j^p[\sin(p\pi/2)\sin(\tau_0)+\cos(p\pi/2)\cos(\tau_0)]}{2}, & i=j.\end{cases} \tag{22}$$

Substitute the system original parameters, and equation (22) becomes

$$[M_{11}]_{ij}^p = \begin{cases} 0, & i\neq j, \\ \dfrac{F_p\omega^p j^p[\cos((p\pi/2)-\omega\tau_1)]}{2}, & i=j.\end{cases} \tag{23}$$

Similarly, the explicit expressions of the other matrices in equation (14) also could be derived. M_2^p and R_2^p are as follows:

$$
\begin{aligned}
&[M_{11}]_{ij}^{p} = \delta_{ij} F_p \omega^p \frac{i^p}{2} \cos\left(\frac{p\pi}{2} - \omega\tau_1\right), \quad i = 0, 1, \ldots, N, j = 0, 1, \ldots, N, \\
&[M_{12}]_{ij}^{p} = \delta_{ij} F_p \omega^p \frac{i^p}{2} \sin\left(\frac{p\pi}{2} - \omega\tau_1\right), \quad i = 0, 1, \ldots, N, j = 1, \ldots, N, \\
&[M_{22}]_{ij}^{p} = \delta_{ij} F_p \omega^p \frac{i^p}{2} \cos\left(\frac{p\pi}{2} - \omega\tau_1\right), \quad i = 1, \ldots, N, j = 1, \ldots, N, \\
&R_{200}^{p} = 0, \\
&R_{21i}^{p} = -F_p \omega^p \left[a_i \frac{i^p}{2} \cos\left(\frac{p\pi}{2} - \omega\tau_1\right) + b_i \frac{i^p}{2} \sin\left(\frac{p\pi}{2} - \omega\tau_1\right) \right], \quad i = 1, \ldots, N, \\
&R_{22i}^{p} = -F_p \omega^p \left[-a_i \frac{i^p}{2} \sin\left(\frac{p\pi}{2} - \omega\tau_1\right) + b_i \frac{i^p}{2} \cos\left(\frac{p\pi}{2} - \omega\tau_1\right) \right], \quad i = 1, \ldots, N,
\end{aligned}
\tag{24}
$$

where δ_{ij} is Kronecker's notation.

$$
\delta_{ij} = \begin{cases} 0, \text{if} & i \neq j, \\ 1, \text{if} & i = j. \end{cases} \tag{25}
$$

Based on equations (12a)–(12g) and (24), the higher-order approximate analytical result of the strongly nonlinear system with parametric excitation and multifrequency excitation under fractional-order delayed feedback could be obtained. When time delay τ_1 is 0, the explicit expression forms of equations (12a)–(12g) and (24) are the same as the explicit forms of the fractional-order derivative in Reference [28], so the correctness of the general formulas in this paper is proved indirectly. By providing the initial value of A_0, ΔA can be obtained through iteration. Then the initial value A_0 of the next iteration would be get, and so on. Repeat iteration until the accuracy of ΔA meets the requirement.

3. Comparison between IHBM and Numerical Integration

In order to analyze the general formulas more correctly, the numerical integration method (NIM) is introduced to simulate equation (1). The numerical calculation form of fractional-order derivative [1, 2] is

$$
D^p[x(t_l)] \approx h^{-p} \sum_{j=0}^{l} C_j^p x(t_{l-j}), \tag{26}
$$

where $t_l = lh$, h is the sample step of calculation, and C_j^p is the binomial coefficient which satisfies the following iterative relationship:

$$
\begin{aligned}
&C_0^p = 1, \\
&C_j^p = \left(1 - \frac{1+p}{j}\right) C_{j-1}^p.
\end{aligned}
\tag{27}
$$

Fractional-order delayed feedback involves time delay τ_1 in equation (1). Let $\tau_1 = i \times h$, i is the natural number and then the fractional-order delayed derivative can be written as

$$
D^p[x(t-\tau_1)] = D^p[x(t-ih)]. \tag{28}
$$

According to equations (26)–(28), the numerical iterative algorithm of equation (1) can be expressed as

$$
\begin{aligned}
&Z_1(t_l) = Z_2(t_{l-1})h - \sum_{j=1}^{l} C_j^1 Z_1(t_{l-j}), \\
&Z_2(t_l) = \begin{bmatrix} F_0 - \sum_{k=1}^{L} F_k \cos(k\omega t_{l-1}) - K_p Z_3(t_{l-1-i}) \\ -\mu Z_2(t_{l-1}) \\ -(1 + 2\varepsilon \cos(\omega t_{l-1})) Z_1(t_{l-1}) \end{bmatrix} h \\
&\qquad - \sum_{j=1}^{l} C_j^1 Z_2(t_{l-j}), \\
&Z_3(t_l) = Z_2(t_{l-1}) h^{1-p} - \sum_{j=1}^{l} C_j^{1-p} Z_3(t_{l-j}),
\end{aligned}
\tag{29}
$$

where $Z_1 = x(t)$, $Z_2 = \dot{x}(t)$, and $Z_3 = D^p[x(t)]$.

Select $L = 3$, and the system external excitation parameters are as follows: $F_0 = 1$, $F_1 = 0.2$, $F_2 = 0.05$, and $F_3 = 0.02$. In the following analysis, the five-order approximately analytical solution is considered, that is to say, the value of N in those general formulas of equations (12a)–(12g) and (24) is selected as 5. Here, we can choose a larger value of N to get a higher precision solution. The solution by NIM is shown by the blue circles based on equation (29). The comparisons between the IHBM results in this paper and the NIM results of equation (1) are shown in Figures 1 and 2. It could be found that the amplitude-frequency curves not only with small parameters but also with large parameters are almost coincided by two methods. Therefore, it could be concluded that the precision of the solution by IHBM in this paper is very high, and it is suitable for both the weakly and the strongly nonlinear fractional-order system. From the observation of the amplitude-frequency curves in Figures 1 and 2, it could be found that there exits two main peaks of the amplitude-frequency curve. The amplitude-frequency curve near $\omega \approx 1$ is the primary resonance response caused by the forcing excitation, and the amplitude-frequency curve near $\omega \approx 0.5$ is the main parametric resonance response caused by the parametric excitation.

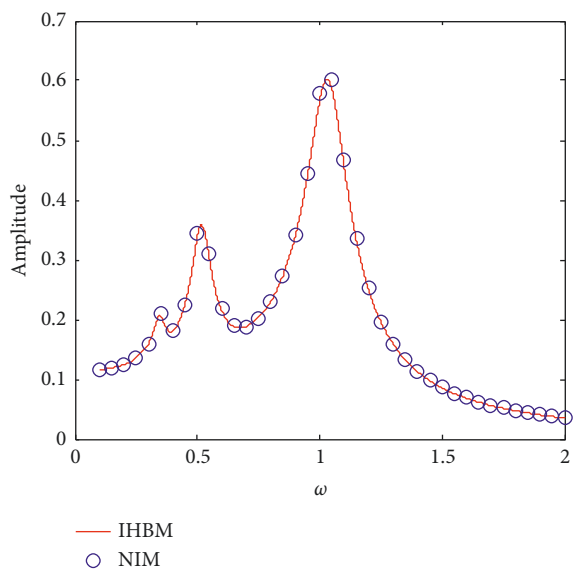

Figure 1: The amplitude-frequency curves with small parameters. ($\mu = 0.1$, $\varepsilon = 0.05$, $Fp = 0.1$, $p = 0.5$, and $\tau_1 = 0.1$).

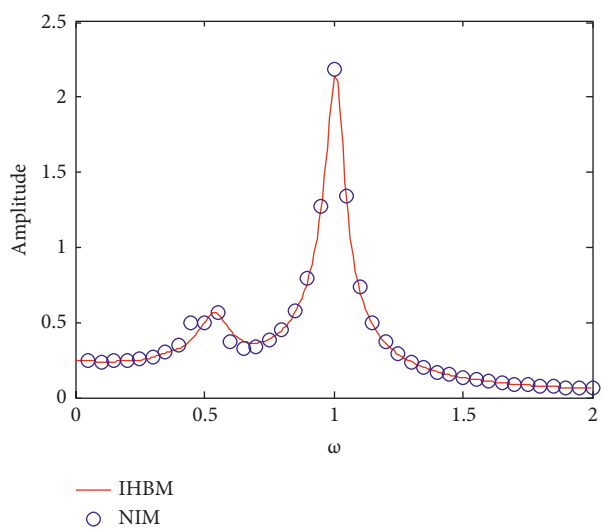

Figure 2: The amplitude-frequency curves with larger parameters. ($\mu = 0.3$, $\varepsilon = 0.2$, $Fp = 0.2$, $p = 0.5$, and $\tau_1 = 2$).

According to the general formulas of IHBM in this paper, the corresponding phase diagrams of $\omega = 1$, $\omega = (1/2)$, and $\omega = (1/3)$ are shown in Figures 3(a)–3(c), respectively, by the red solid line. From the observation of Figure 3, whether in the primary resonance region ($\omega \approx \omega_0$), the main parametric resonance region ($\omega \approx (\omega_0/2)$), or the superharmonic resonance region ($\omega \approx (\omega_0/3)$), it could be found that the solution of equation (1) obtained by IHBM is in good agreement with the solution by NIM. Therefore, for a complex parametric system under multifrequency excitation, the dynamical characteristics of the system in different resonance regions can be simultaneously reflected based on IHBM proposed in this paper.

4. The Effects of the Feedback Control Parameters

4.1. The Effect of the Fractional Order. We have the fractional order from 0 to 2 due to the causality and physical realizability [35], and the amplitude-frequency curves according to the general formulas are obtained, as are shown in Figure 4, where $\mu = 0.1$, $\varepsilon = 0.2$, $F_0 = 1$, $F_1 = 0.2$, $F_2 = 0.05$, $F_3 = 0.02$, $K_p = 0.2$, and $\tau_1 = 0$. The amplitude-frequency curve near $\omega \approx 1$ is the primary resonance response, where the circles represent the maximum amplitude in the primary resonance region with different fractional order, respectively. The amplitude-frequency curve near $\omega \approx 0.5$ is the main parametric resonance response, where the asterisks represent the maximum amplitude in the main parametric resonance region. From the observation of Figure 4, it could be found that the maximum amplitudes show a trend of first decrease and then increase as the increasing of the fractional order ($p \in [0 \;\; 2]$), the largest maximum amplitude appears at $p = 2$, and the smallest maximum amplitude appears at $p = 1$. Simultaneously, one could find that whether in the primary resonance region or in the main parametric resonance region, the increasing of the fractional order p would result into the leftwards moving of the maximum amplitude position. This is because the equivalent linear stiffness from fractional-order delayed feedback will become smaller as the fractional order increase, and the equivalent linear damping from fractional-order delayed feedback will become larger at first and then smaller in this procedure. It can be obtained that the vibration behavior of the system will be restrained with the increasing of the fractional order ($p \in [0 \;\; 1]$). When $p = 1$, the fractional-order delayed feedback is equivalent to the velocity feedback, which brings the maximum damping effect, and at this time the maximum amplitude of the system is minimal.

4.2. The Effect of Time Delay. With the change of time delay ($\tau_1 \in [0 \;\; 4]$), the amplitude-frequency curves are shown in Figure 5, where $\mu = 0.1$, $\varepsilon = 0.2$, $F_0 = 1$, $F_1 = 0.2$, $F_2 = 0.05$, $F_3 = 0.02$, $K_p = 0.2$, and $p = 0.5$. It could be found from Figure 5 that maximum amplitudes firstly increase and then decrease with the increase of time delay in the primary resonance region. But maximum amplitudes constantly increase with the increase of time delay in the main parametric resonance region in this procedure. Whether in the primary resonance region or in the main parametric resonance region, the increase of time delay would firstly result into the rightwards moving and then leftwards moving of the maximum amplitude position. The dynamical phenomena shows that the change of time delay will change the stiffness effect and the damping effect from fractional-order delayed feedback.

When time delay is increased from 0 to 10, the change of the amplitude-frequency curve with the increase of time delay is shown in Figure 6. From Figure 6, with the increase of time delay, maximum amplitudes increase first and then decrease, then increase and decrease, and so on in the resonance region. Those dynamical phenomena is cyclical with the increase of time delay, which could also be obtained from the analysis of

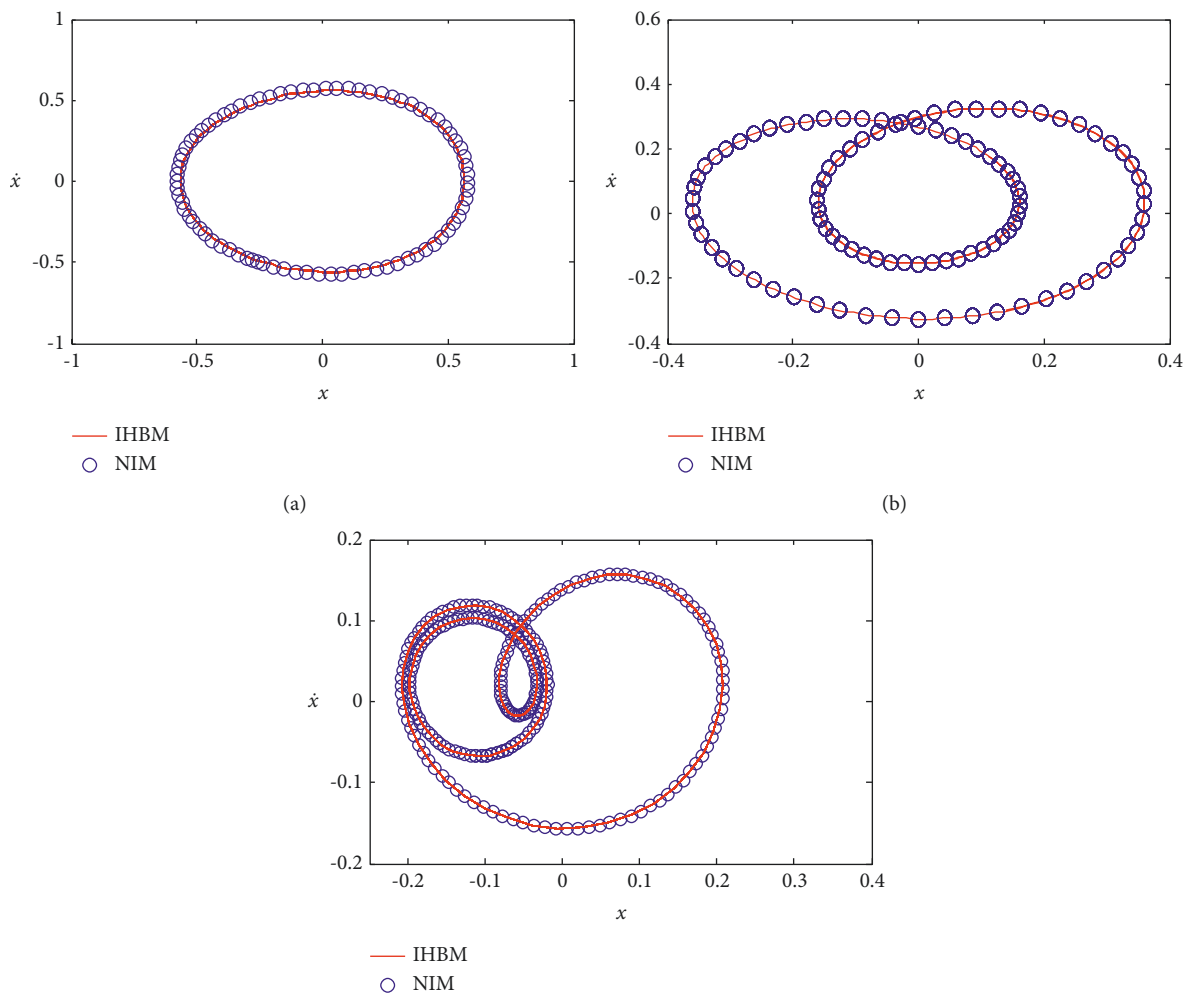

Figure 3: (a) Phase portrait $\omega = 1$ ($\mu = 0.1$, $\varepsilon = 0.05$, $Fp = 0.1$, $p = 0.5$, and $\tau_1 = 0.1$). (b) Phase portrait $\omega = 1/2$ ($\mu = 0.1$, $\varepsilon = 0.05$, $Fp = 0.1$, $p = 0.5$, and $\tau_1 = 0.1$). (c) Phase portrait $\omega = 1/3$ ($\mu = 0.1$, $\varepsilon = 0.05$, $Fp = 0.1$, $p = 0.5$, and $\tau_1 = 0.1$).

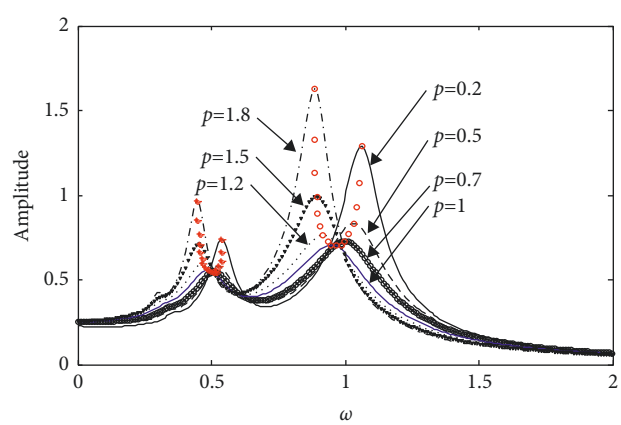

Figure 4: The amplitude-frequency curves.

the general formulas of equation (24). Through the analysis of equation (24), we could find that time delay affects the dynamic characteristics of the system in the form of trigonometric function. Therefore, it can be inferred that the dynamical phenomena is also cyclical with the increase of time delay in the parametric resonance region. Because of the difference of the resonance frequency between the primary resonance and the parametric resonance, the period of cycle

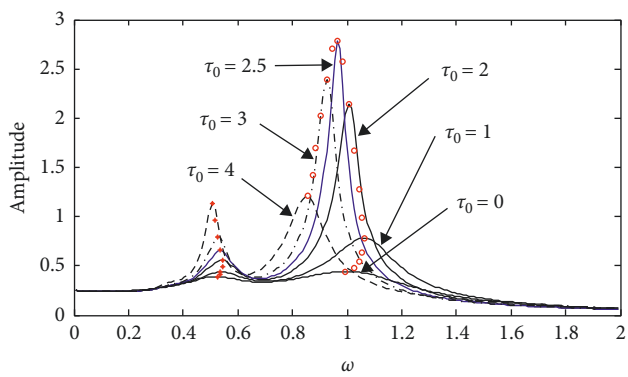

Figure 5: The amplitude-frequency curves.

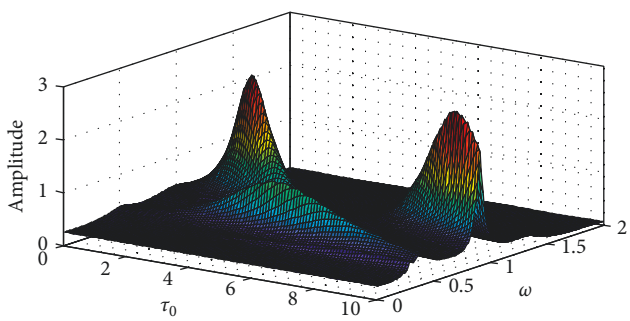

Figure 6: The amplitude-frequency-delay graph.

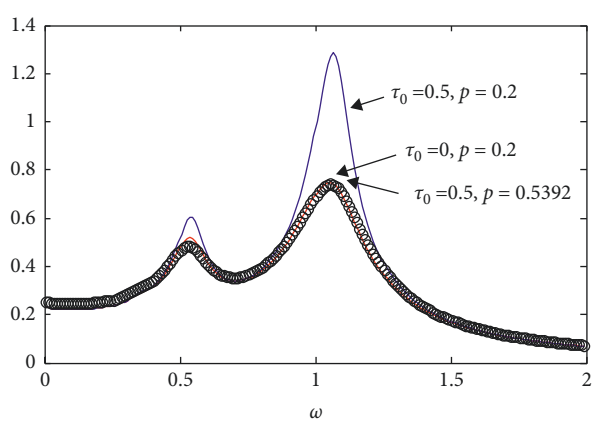

Figure 7: The amplitude-frequency curves.

of the primary resonance motion response is faster than the parametric resonance motion response. Vibration amplitudes in different resonance regions can be reduced by choosing appropriate time delay. Those results will help us to design the parameters of fractional-order delayed feedback in the Mathieu equation with multifrequency excitation.

From the analysis of equation (24), it could be found that the fractional order affects the dynamical characteristics of the system in the form of trigonometric function too. A reasonable choice of the fractional order can offset the complex dynamical problem caused by time delay. The equation of the fractional order and time delay relation is

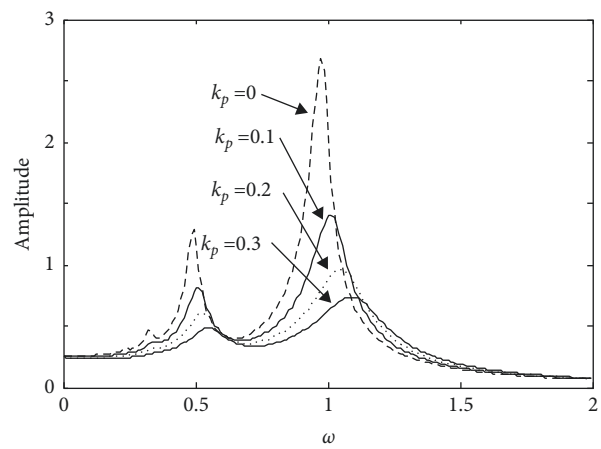

Figure 8: The amplitude-frequency curves.

$$\Delta p = \frac{2\omega\tau_0}{\pi}. \tag{30}$$

Select $\mu = 0.1$, $\varepsilon = 0.2$, $F_0 = 1$, $F_1 = 0.2$, $F_2 = 0.05$, $F_3 = 0.02$, and $K_p = 0.2$. When $p = 0.2$ and $\tau_0 = 0$, the amplitude-frequency curve is shown in Figure 7 by the red solid line. From the comparison of the two curves, it could be found that maximum amplitudes become larger both in the primary resonance region and in the parametric resonance region when time delay is 0.5. Substituting $\tau_0 = 0.5$ into equation (30), we can get $\Delta p \approx 0.3392$. Let the fractional order $p = 0.2 + 0.3392 = 0.5392$, and the amplitude-frequency curve is shown in Figure 7 by circles. It could be found that those circles almost coincided with the red solid line. Therefore, it can be inferred that the appropriate fractional order can offset the effect of time delay. When time delay is disadvantageous, the complex dynamical problem of the system caused by time delay can be eliminated through selecting different viscoelastic components. This will provide a new design idea for the control strategy of the system.

4.3. The Effect of the Feedback Gain Coefficient. When the feedback gain coefficient F_p is changed, the amplitude-frequency curves are obtained as are shown in Figure 8, where $\mu = 0.1$, $\varepsilon = 0.2$, $F_0 = 1$, $F_1 = 0.2$, $F_2 = 0.05$, $F_3 = 0.02$, $p = 0.5$, and $\tau_1 = 0.2$. From the observation of Figure 8, it could be found that maximum amplitudes decrease both in the primary resonance region and in the parametric resonance region with the increase of the feedback gain coefficient F_p. The amplitude-frequency curve near $\omega \approx 0.3$ represents the superharmonic resonance response, which will disappear with the larger of the feedback gain coefficient in this region. It can be concluded that the feedback gain coefficient can suppress the maximum vibration amplitude of the system. The resonance frequency in each resonance region is moved to the right with the increase of the feedback gain coefficient. It is shown that the increase of the feedback gain coefficient can increase both the equivalent linear damping and the equivalent linear stiffness of the system.

5. Conclusion

In this paper, the complex dynamical characteristics of the Mathieu equation with multifrequency excitation under fractional-order delayed feedback control are investigated by IHBM. At first, the general formulas of the approximate analytical solution for this system is obtained. The more accurate solution could be obtained through using the obtained general formulas. Then, the numerical result of this system is also studied. The comparison between the result by NIM and the approximate analytical solution by IHBM is given, and the correctness precision of the general forms of the approximate analytical solution is verified. At last, the effects of fractional-order delayed feedback are investigated. Both the fractional order and time delay of fractional-order delayed feedback will affect the dynamical response of the system in the form of trigonometric function. The appropriate fractional order can offset the disadvantageous dynamical problem caused by time delay. The feedback gain coefficient can suppress the maximum vibration amplitude of the system, and so on. Those results could help us to design the control parameters of fractional-order delayed feedback in the Mathieu equation with multifrequency excitation. It can also provide beneficial reference for other fractional-order control systems, even for the strongly nonlinear systems.

Data Availability

The data used to support the findings of this study are included within the article.

Conflicts of Interest

The authors declare that they have no conflicts of interest.

Acknowledgments

The authors are grateful to the support by the National Natural Science Foundation of China (12072206, U1934201, and 11802183) and the Education Department Project of Hebei Province (ZD2020310).

References

[1] I. Petras, *Fractional-Order Nonlinear Systems: Modeling, Analysis and Simulation*, Higher Education Press, Beijing, China, 2011.

[2] H. Singh, D. Kumar, and D. Baleanu, *Methods of Mathematical Modelling: Fractional Differential Equations*, CRC Press, Boca Raton, FL, USA, 2019.

[3] C. I. Muresan, P. Ostalczyk, and M. D. Ortigueira, "Fractional calculus applications in modeling and design of control systems," *Journal of Applied Nonlinear Dynamics*, vol. 6, no. 2, pp. 131–134, 2017.

[4] M. Gholami, R. K. Ghaziani, and Z. Eskandari, "Three-dimensional fractional system with the stability condition and chaos control," *Mathematical Modelling and Numerical Simulation with Applications*, vol. 2, no. 1, pp. 41–47, 2022.

[5] A. Ebaid, E. R. El-Zahar, A. F. Aljohani, B. Salah, M. Krid, and J. T. Machado, "Analysis of the two-dimensional fractional projectile motion in view of the experimental data," *Nonlinear Dynamics*, vol. 97, no. 2, pp. 1711–1720, 2019.

[6] Y. G. Yang and W. Xu, "Stochastic analysis of monostable vibration energy harvesters with fractional derivative damping under Gaussian white noise excitation," *Nonlinear Dynamics*, vol. 94, no. 1, pp. 639–648, 2018.

[7] H. G. Sun, Y. Zhang, D. Baleanu, W. Chen, and Y. Q. Chen, "A new collection of real world applications of fractional calculus in science and engineering," *Communications in Nonlinear Science and Numerical Simulation*, vol. 64, pp. 213–231, 2018.

[8] J. Trigeassou and N. Maamri, *Analysis, Modeling, and Stability of Fractional Order Differential Systems*, Wliey, New York, NY, USA, 2019.

[9] E. R. El-Zahar, A. M. Alotaibi, A. Ebaid, A. Aljohani, and J. Gómez Aguilar, "The Riemann-Liouville fractional derivative for Ambartsumian equation," *Results in Physics*, vol. 19, Article ID 103551, 2020.

[10] A. Ebaid, C. Cattani, A. S. Al Juhani, and E. R. El-Zahar, "A novel exact solution for the fractional Ambartsumian equation," *Advances in Difference Equations*, vol. 2021, no. 1, p. 88, 2021.

[11] Z. H. Wang and H. Y. Hu, "Stability of a linear oscillator with damping force of the fractional-order derivative," *Science China Physics, Mechanics & Astronomy*, vol. 53, no. 2, pp. 345–352, 2010.

[12] Y. J. Yu and Z. H. Wang, "Initial state dependent nonsmooth bifurcations in a fractional-order memristive circuit," *International Journal of Bifurcation and Chaos*, vol. 28, Article ID 1850091, 2018.

[13] J. Trigeassou, N. Maamri, J. Sabatier, and A. Oustaloup, "A Lyapunov approach to the stability of fractional differential equations," *Signal Processing*, vol. 91, no. 3, pp. 437–445, 2011.

[14] C. P. Li, A. Chen, and J. J. Ye, "Numerical approaches to fractional calculus and fractional ordinary differential equation," *Journal of Computational Physics*, vol. 230, no. 9, pp. 3352–3368, 2011.

[15] C. P. Li and A. Chen, "Numerical methods for fractional partial differential equations," *International Journal of Computer Mathematics*, vol. 95, no. 6-7, pp. 1048–1099, 2017.

[16] A. Ebaid and H. K. Al-Jeaid, "The mittag-leffler Functions for a Class of first-order fractional initial value problems: dual Solution via riemann-liouville fractional derivative," *Fractal and Fractional*, vol. 6, no. 2, p. 85, 2022.

[17] G. Failla and A. Pirrotta, "On the stochastic response of a fractionally-damped Duffing oscillator," *Communications in Nonlinear Science and Numerical Simulation*, vol. 17, no. 12, pp. 5131–5142, 2012.

[18] Y. J. Shen, S. F. Wen, X. H. Li, S. P. Yang, and H. J. Xing, "Dynamical analysis of fractional-order nonlinear oscillator by incremental harmonic balance method," *Nonlinear Dynamics*, vol. 85, no. 3, pp. 1457–1467, 2016.

[19] S. F. Wen, Y. J. Shen, S. P. Yang, and J. Wang, "Dynamical response of Mathieu-Duffing oscillator with fractional-order delayed feedback," *Chaos, Solitons & Fractals*, vol. 94, pp. 54–62, 2017.

[20] A. Y. T. Leung and S. K. Chui, "Non-linear vibration of coupled duffing oscillators by an improved incremental harmonic balance method," *Journal of Sound and Vibration*, vol. 181, no. 4, pp. 619–633, 1995.

[21] W. Liu, Z. Guo, and X. Yin, "Stochastic averaging for SDOF strongly nonlinear system under combined harmonic and

Poisson white noise excitations," *International Journal of Non-linear Mechanics*, vol. 126, no. 1, Article ID 103574, 2020.

[22] H. Yuda, H. Peng, and Z. Jinzhi, "Strongly nonlinear subharmonic resonance and chaotic motion of axially moving thin plate in magnetic field," *Journal of Computational and Nonlinear Dynamics*, vol. 10, no. 2, Article ID 021010, 2015.

[23] Z. Odibat and A. Sami Bataineh, "An adaptation of homotopy analysis method for reliable treatment of strongly nonlinear problems: construction of homotopy polynomials," *Mathematical Methods in the Applied Sciences*, vol. 38, no. 5, pp. 991–1000, 2015.

[24] N. Perchikov and O. V. Gendelman, "Transient dynamics in strongly nonlinear systems: optimization of initial conditions on the resonant manifold," *Philosophical Transactions of the Royal Society A: Mathematical, Physical & Engineering Sciences*, vol. 376, no. 2127, Article ID 20170131, 2018.

[25] K. W. Chung, C. L. Chan, Z. Xu, and G. M. Mahmoud, "A perturbation-incremental method for strongly nonlinear autonomous oscillators with many degrees of freedom," *Nonlinear Dynamics*, vol. 28, no. 3/4, pp. 243–259, 2002.

[26] S. L. Lau and W. S. Zhang, "Nonlinear vibrations of piecewise-linear systems by incremental harmonic balance method," *Journal of Applied Mechanics*, vol. 59, no. 1, pp. 153–160, 1992.

[27] L. Xu, M. Lu, and Q. Cao, "Nonlinear vibrations of dynamical systems with a general form of piecewise-linear viscous damping by incremental harmonic balance method," *Physics Letters A*, vol. 301, no. 1-2, pp. 65–73, 2002.

[28] S. F. Wen, Y. J. Shen, X. N. Wang, S. P. Yang, and H. J. Xing, "Dynamical analysis of strongly nonlinear fractional-order Mathieu-Duffing equation," *Chaos: An Interdisciplinary Journal of Nonlinear Science*, vol. 26, no. 8, Article ID 084309, 2016.

[29] N. Chen, N. Chen, and Y. Chen, "The fractional-order control method for four-wheel steering system," *Science China*, vol. 40, no. 2, pp. 139–144, 2010.

[30] L. C. Chen, F. Hu, and W. Q. Zhu, "Stochastic dynamics and fractional optimal control of quasi integrable Hamiltonian systems with fractional derivative damping," *Fractional Calculus and Applied Analysis*, vol. 16, no. 1, pp. 189–225, 2013.

[31] D. Avci, N. Ozdemir, and M. Yavuz, "Fractional optimal control of diffusive transport acting on a spherical region," *Methods of Mathematical Modelling*, CRC Press, Boca Raton, FL, USA, 2019.

[32] Q. X. Liu, J. K. Liu, and Y. M. Chen, "Alternate stability switches induced by time delay in nonlinear fractional oscillators," *International Journal of Non-linear Mechanics*, vol. 116, pp. 55–61, 2019.

[33] G. M. Bahaa, "Optimal control problem for variable-order fractional differential systems with time delay involving Atangana-Baleanu derivatives," *Chaos, Solitons & Fractals*, vol. 122, pp. 129–142, 2019.

[34] C. D. Huang, H. Liu, X. P. Chen, M. S. Zhang, and A. DingCaoAlsaedi, "Dynamic optimal control of enhancing feedback treatment for a delayed fractional order predator-prey model," *Physica A: Statistical Mechanics and Its Applications*, vol. 554, Article ID 124136, 2020.

[35] C. W. De Silva, *Modeling of Dynamic Systems with Engineering Applications*, CRC Press, Boca Raton, FL, USA, 2017.